

Green Synthesis of Mediated Ag/MgO Nanohydroxyapatite from Crayfish Using Orange Peel Extract (*Citrus aurantium delcis*)for BiomaterialsApplications

Damilola Esther Afolabi¹, Adeyinka Ademilua², Daniel Ayodele Idowu³

^{1,2,3} Department of Chemistry, Federal University of Agriculture, Abeokuta, Ogun State, Nigeria
ademiluaadeyinka62@gmail.com



This is an open-access article distributed under the terms of the [Creative Commons Attribution 4.0 International License](https://creativecommons.org/licenses/by/4.0/), which permits unrestricted use, distribution, and reproduction in any medium, provided the original work is properly cited.

Abstract-Conversion of waste such as crayfish shell to resourceful biomaterial like Hydroxyapatite is a led-light to the realization of United Nation vision 2030.Waste crayfish shell are being generated in tons of million across the globe annually thus constituting environmental pollution, while the demand for the synthesis of pure and biologically active materials is on the increase. This present work is aimed at investigating the facile synthesis of crayfish waste derived hydroxyapatite (CFSHAP) and substituent synthesis of its orange peel extract mediated Ag/MgOnHAP nanocomposite, as a potential biomaterial in bone tissue engineering application. The phase purity, composition, size, functional groups and surface morphology of the apatite were elucidated using spectroscopic (X-ray Diffraction (XRD); Fourier Transform Infrared Spectroscopy (FR-IR) and Scanning Electron Microscopy). The results SEM showed that Ag/MgO- CFSHAP nanoparticles have round morphologies and the SEM-EDS revealed the characteristic Ag, Mg, Ca/P and O composition, FT-IR analysis confirmed relevant hydroxylapatite functional groups like carbonate, phosphate and hydroxyl groups while XRD analysis revealed a well crystalline monophasic HAp powder comparabile to the MAP reference model (JCPDF no. 00-064-0738). The 1000^oc calcined Ag/MgO-CFSHAP also displayed stable phase stability which could lead to increased densification and porosity. The use of Ag will introduce antibacterial properties, while MgO will introduce osseointegration into the HAp

Keywords: Hydroxylapatite, Crayfish Shell, Biomaterials, Nanoparticles, Tissue Engineering, Osseointegration.

Introduction

The word, nanotechnology, which is said to be the control of the materials at the atomic, molecular, and supramolecular level, is considered as the production and integration of nanoparticles (NPs) in many areas such as food, agriculture, technology, and industry (Agarwal et al., 2017; Singh et al., 2018). It can be categorized into different types like metal NPs (e.g. Fe and Ag), metal oxide NPs (e.g. CuO), carbon-based NPs, lipid-based NPs, and quantum dots (Elshama et al., 2018). In past years, research on the usability and application of metal oxide nanoparticles in the field of health has dramatically increased with major innovations. Although, these metal oxide NPs are prepared by different methods such as chemical, physical, or biological approaches, giving rise to metal oxide NPs obtained by biogenic reduction which attract more attention in this field, where purity is an important criterion (Hussain et al., 2016; Erdogan et al., 2019). In these field, physical methods such as pulsed laser deposition and molecular beam epitaxy have disadvantages such as being more expensive and the need for qualified laboratories (Lastra et al., 2014; Ozgur et al., 2018). Since these methods of using chemical reducing compounds are altered by a naturally reducing product, metal oxide NPs synthesized with a green approach are free of chemical contaminants. Moreover, they are eco and bio-friendly, easily recyclable, and less expensive (Bandeira et al., 2020; Sultana et al., 2020). The biological activities of green-synthesized metal oxide NPs have also been reported to be higher compared to chemically synthesized metal oxide NPs (Ganaie et al., 2019).

Synthetic hydroxyapatite is majorly utilized as effective and efficiently material for repairing damaged teeth and bones, drug delivery agent and dental applications as a result of its resemblance with key mineral constituent of hard tissue in human body which is as a result of its excellent osteoconductivity, biocompatibility and bioactivity (Dennymol et al., 2014; Shin-ching et al., 2016; Tang et al., 2019; Li et al., 2018). Also, variety of chemical reactions utilized fabricated hydroxyapatite (HAp) as a possible adsorbent, catalyst or as a catalyst support (Shin-ching et al., 2016; Shi et al., 2021). Besides, hydroxyapatite powder can as well be used as an excellent adsorbent for the remediation of metals and organic contaminants due to its strong adsorptive property (Ofudje et al., 2021). Synthesis of non-stoichiometric apatite for biomaterial applications is on the high since pure apatite only co-exists with its derivatives in any biological system (Doan et al., 2014; Muthu et al., 2020). Substituted hydroxyapatite are formed via chemical substitution of calcium ions (Ca^{2+}), phosphate (PO_4^{3-}) or hydroxyl (OH^-) with other ions such as F^- , Na^+ , Mg^{2+} , K^+ , Cl^- , and CO_3^{2-} . Recently, biological derived hydroxyapatite from the components of natural materials such as bone, shell and plants have been documented in literature (Shih-ching et al., 2016; Muthu et al., 2020; Guerrero et al., 2017; Hamidi et al., 2017; Toibah et al., 2019). For instance, Shih-Ching et al., (2016) reported the formation of HAp phase via ballmilling followed by calcinations to form a biphasic calcium phosphate after 5 h of ball milling and 1 h of heat treatment at 1000 °C. Also, Habeeb and Salih., (2024) described the used of calcium oxide from eggshell which was calcined at 1000 °C and reacted with phosphoric acid in ratio 1:1 to produced HAp through mechanical milling. Leyla et al., (2023) adsorbed heavy metal with hydroxyapatite with the same precursor in ratio 1:2 via precipitation method. Higher crystallinity and smaller particles size with HAp from eggshell were found by (Sandile et al., 2023) when compared with HAp extracted from fish scales. Though, there have been reports on the synthesis of hydroxyapatite powder from waste agro-materials as mentioned above, the

fabrication of porous scaffold nano-composite to enhance the cell diffusion during implant and the detailed study of their toxicity has not been well explored. Thus, this work tends to utilize agro-waste for the production of porous scaffold hydroxyapatite-ammonium bicarbonate nano-composite. Therefore, this study aimed to fabricate HAp derived from crayfish for potential application in biomaterials applications.

2.0 Materials And Methods

2.1 Materials

The calcium hydroxide $\text{Ca}(\text{OH})_2$, Ammonium dihydrogen phosphate $(\text{NH}_4)\text{H}_2\text{PO}_4$, Ammonium solution, Distilled water used for this investigation are in analytical grades and were used without further purification.

2.2. Preparation of Citrus aurantium delcisPeel Extract.

Fresh collected orange fruits were washed with distilled water to remove visible unwanted particles from the surface. The oranges were peeled and cut into small pieces, and the weight was recorded. The sample was sun-dried at the initially to naturally reduce some amount of moisture content from the orange peels after which the sample was then dried in an oven for 8 h at a temperature of 60°C , and the weight was recorded. The dried sample were then ground into a fine powder using a hand mill, and the weight obtained. 20 g of the powdered sample was dispersed in 300 mL of distilled water in a beaker. The prepared solution was stirred continuously for 3 h with a magnetic stirrer to ensure a uniform mixture of the solution. The mixture was then subjected to a water bath at 60°C for 1 h. The solution was then filtered using Whatman filter paper to obtain the orange peel extract, which was stored in a refrigerator (Amanulla and Sundaram, 2019; Kumar et al., 2020).

2.3 Preparation of Calcium Oxide From Crayfish Mandible Source

Uncrushed crayfish mandible were obtained from Olomoo fish market in Abeokuta, Ogun State. The raw material was boiled for 30 mins with distilled water and filtered. After boiling, the crayfish sample was sun-dried for 3 days and then oven dried at 100°C overnight. The dried sample was crushed into smaller pieces using an electric blender. Crayfish were then calcined in a muffle furnace at a temperature of a rate of $5^\circ\text{C}/\text{min}$ in three stages of calcination. The temperature was maintained for 3 h to remove the organic matrix and for the decomposition of calcium carbonate into calcium oxide. The powders were cooled at room temperature by slow furnace cooling and kept for the synthesis of hydroxyapatite carbonate into calcium oxide. The CaO powder were cooled at room temperature by slow furnace cooling and kept for the synthesis of hydroxyapatite.

2.4 Synthesis of Ag/Mgo Cfhap

0.75 M solution of $\text{Ca}(\text{OH})_2$ was obtained into 100 mL of distilled water in a 500 mL beaker and placed on hot plate and stirred for 30 mins with a magnetic stirrer. 100 mL of prepared 0.45 M of ammonium dihydrogen phosphate $(\text{NH}_4)\text{H}_2\text{PO}_4$, filtrate of silver and magnesium oxide from

orange peel extract was added drop wise and stirred for about 30mins. The pH of the solution was adjusted to 10 by using ammonia solution. The mixture was left for 24h on the magnetic stirrer at room temperature for the formation of hydroxylapatite and thereafter filtered and centrifuged at 4000rpm for 15mins and washed with distilled water to remove excess ammonia solution. The powder was dried in an oven and the solid particles formed were turned into CFHAp.

2.5 Synthesis Of Ag-Mgo Nanohydroxylapatite Composite

Modified functionalized nanohydroxyapatite bound to Ag-MgO nanoparticles was synthesized using a combination of procedures (Poinern et al., 2011; Sushma et al., 2016). The experimental procedure entails seed growth via bio-reduction and precipitation method at room temperature using a natural mild natural reducing agent (aqueous *C. aurantium* peel extracts) in the presence of other metallic precursors. Briefly, a homogeneous aqueous mixture of bio-reduced Ag-MgO nanoparticles using a natural reductant agent was obtained from an optimized microwave-assisted aqueous mixture of *C. aurantium* Peel extracts/1 mM AgNO₃ (2:3 v/v %) mixed with 20 mL 0.1 M (Mg(NO₃)₂.6H₂O) under continuous stirring for 2 h at room temperature with 2 mL 0.2M Ammonia solution added drop wise until a complete precipitation was achieved. The Ag-MgO mixture thus obtained was added to 40 mL 0.32 M CaO and 100M (NH₄)H₂PO₄ solution (Ca/Pt 1.67) under continuous stirring. Subsequently, NH₄OH (25%) was added drop wise to adjust the pH value to 9, and the solution was stirred for another 2 hours. During the mixing process; the pH value was continually checked and maintained at 9 (using NH₄OH). The composite solution was thereafter subjected to ultrasound agitation at 100% amplitude(0.5 cycles) for 1 h. The product obtained after the sonication was filtered and dried at 40 °C in an oven for 24 h before being ground into a fine powder.

2.6 Characterization and Instrumentation

The characterization study of silver nanoparticles was done by examining the size, shape and quantity of particles. Several number of techniques was used for this purpose,among which are Uv-Vis spectroscopy (UV), Scanning Electron Microscopy (SEM),X-ray Diffraction (XRD),Fourier Transmission Infrared Spectroscopy (FTIR).

3.Result And Discussion

3.1 Biosynthesis of Control-HAp and Orange peel extract -HAp from crayfish source

HAp was biosynthesized using crayfish as substrate. The control HAp synthesized from crayfish without the incorporation of peel extract was whitish in color, and in liquid form. Incorporation of orange peel extracts during the synthesis of HAp was done to serve as a reducing agent and to provide antimicrobial properties to the synthesized biopolymer. OPE-HAp obtained through the green synthesis method was greenish in color, and in powder form. The green synthesized HAp was reported to have greater crystallinity and stability as compared to chemically synthesized HAp. This fact can be attributed to the presence of reactive functional groups in plant polyphenolsacts as precursors and aids in calcium - chelate formation. This complex further

reacts with phosphate precursor to initiate the nucleation process resulting in HAp biosynthesis (Alorku et al., 2020). The green synthesis method further improves the functional properties like antimicrobial and antioxidant activity majorly contributed by the phytochemicals present in the plant extract (Ibraheem et al 2019).

4.2. Fourier transform-infrared (FT-IR) analysis

FTIR analysis was carried out for investigating the functional groups present in HAp for its structural elucidation and responsible for the formation of the nanocomposite.

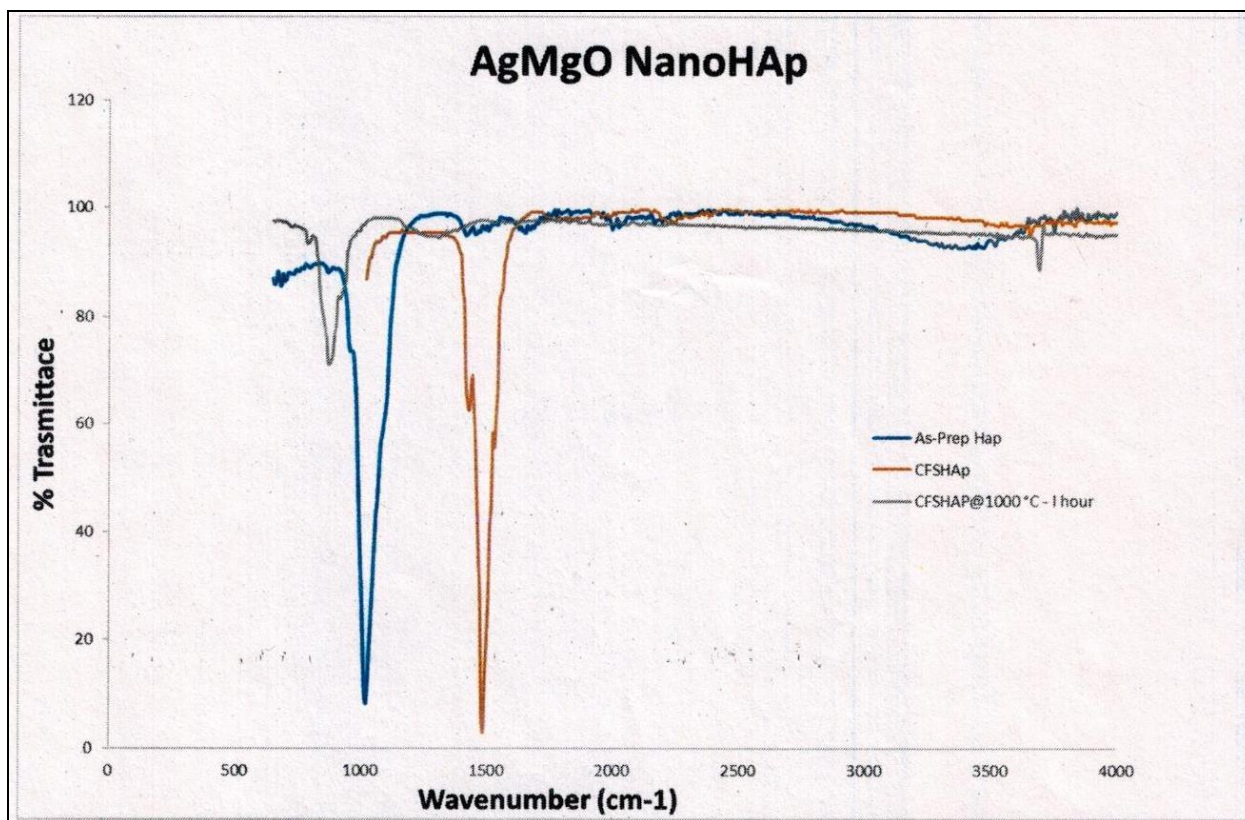


Figure 1: FT-IR Spectrum of the Ag/MgO Nanohydroxyapatite

The FTIR spectrum of the Ag/MgO nanohydroxyapatite composite (Figure 1) revealed several characteristic absorption bands indicative of both hydroxyapatite structure and bio-organic residues from the orange peel extract used in the green synthesis. A broad absorption band observed around 3290 cm⁻¹ corresponds to O–H stretching vibrations, which is associated with structural hydroxyl groups in the hydroxyapatite lattice and adsorbed water molecules. Bands appearing between 1638 and 1645 cm⁻¹ are attributed to H–O–H bending modes of molecular water. These bands indicate residual moisture or lattice water, in agreement with the hydrated nature of biologically derived hydroxyapatite. Absorptions within the 2000–2380 cm⁻¹ range reflect C≡C and C≡N stretching, possibly originating from secondary metabolites like flavonoids or alkaloids present in the orange peel extract. These phytochemicals act as bio-reductants and stabilizers during nanoparticle formation. An absorption spectrum observed around 1040–1100

cm^{-1} corresponds to PO_4^{3-} asymmetric stretching modes, a hallmark of phosphate groups in hydroxyapatite. Also, the presence of carbonate bands (CO_3^{2-}) is expected around 880 cm^{-1} and 1456 cm^{-1} , suggesting B-type carbonated hydroxyapatite, where carbonate ions substitute phosphate groups. The combination of hydroxyl, phosphate, and carbonate functional groups confirms the successful formation of a nanocrystalline hydroxyapatite phase. It should be noted that the additional peaks assigned to phenolic, amine, or flavonoid-like groups highlight the role of the orange peel extract not only in nanoparticle reduction and stabilization but also in conferring bioactivity and antimicrobial potential to the composite. However, the appearance of the bands in the range of $3452\text{--}3572 \text{ cm}^{-1}$ evidently confirmed the presence of hydroxyl group of the hydroxyapatite (Adak and Purohit, 2011; Agalya et al., 2022).

4.3 Xrd Analysis

The XRD pattern of the synthesized Ag/MgO-CFHAp nanocomposite (Figure 2 & 3) displayed sharp and well-defined diffraction peaks characteristic of crystalline hydroxyapatite. Notably, the most intense peaks appear at $2\theta = 25.88^\circ$ and 32.20° , corresponding to the (002) and (112) planes respectively. These peak positions and their relative intensities closely match those in the standard hydroxyapatite reference file (JCPDS No. 00-064-0738), thereby confirming the successful formation of the hexagonal HAp phase. The presence of additional peaks at 22.86° , 38.18° , 40.45° , and 46.70° corresponding to the (111), (200), (220), (221), and (222) planes indicate secondary crystalline phases assigned to face-centered cubic (fcc) silver (Ag) and magnesium oxide (MgO). These diffraction features confirm the incorporation of Ag and MgO nanoparticles into the hydroxyapatite matrix, thus forming a multiphase composite material. (Oladoyinbo et al., 2024).

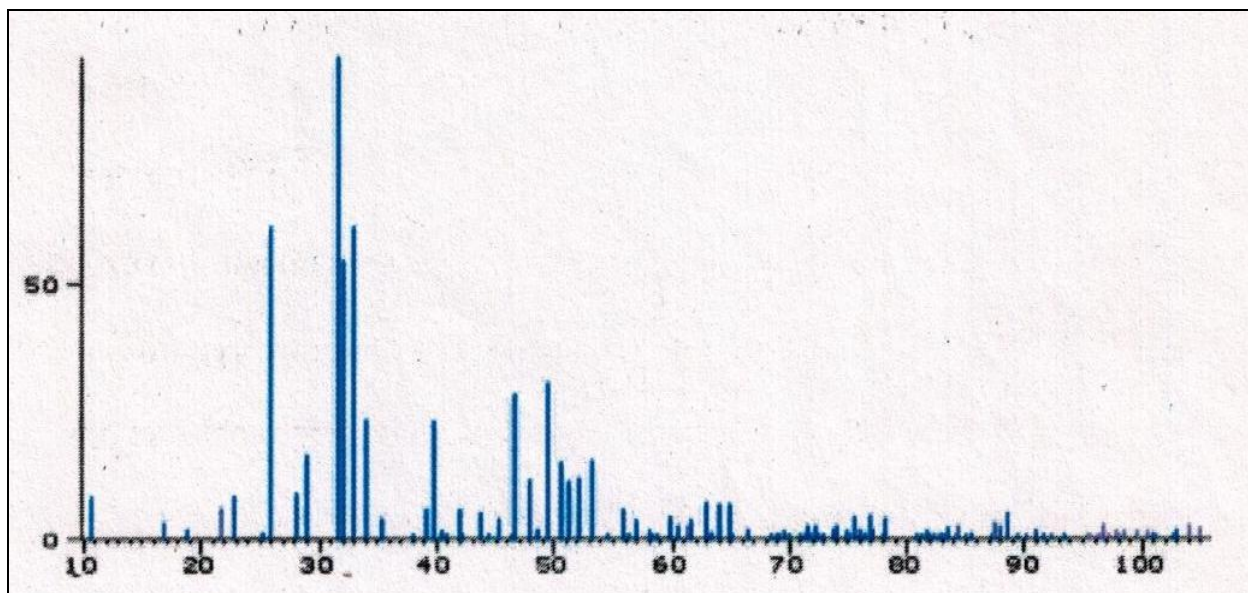


Figure 2: XRD Diffractogram of HAp Reference Model (JCPDF NO. 00-064-0738)

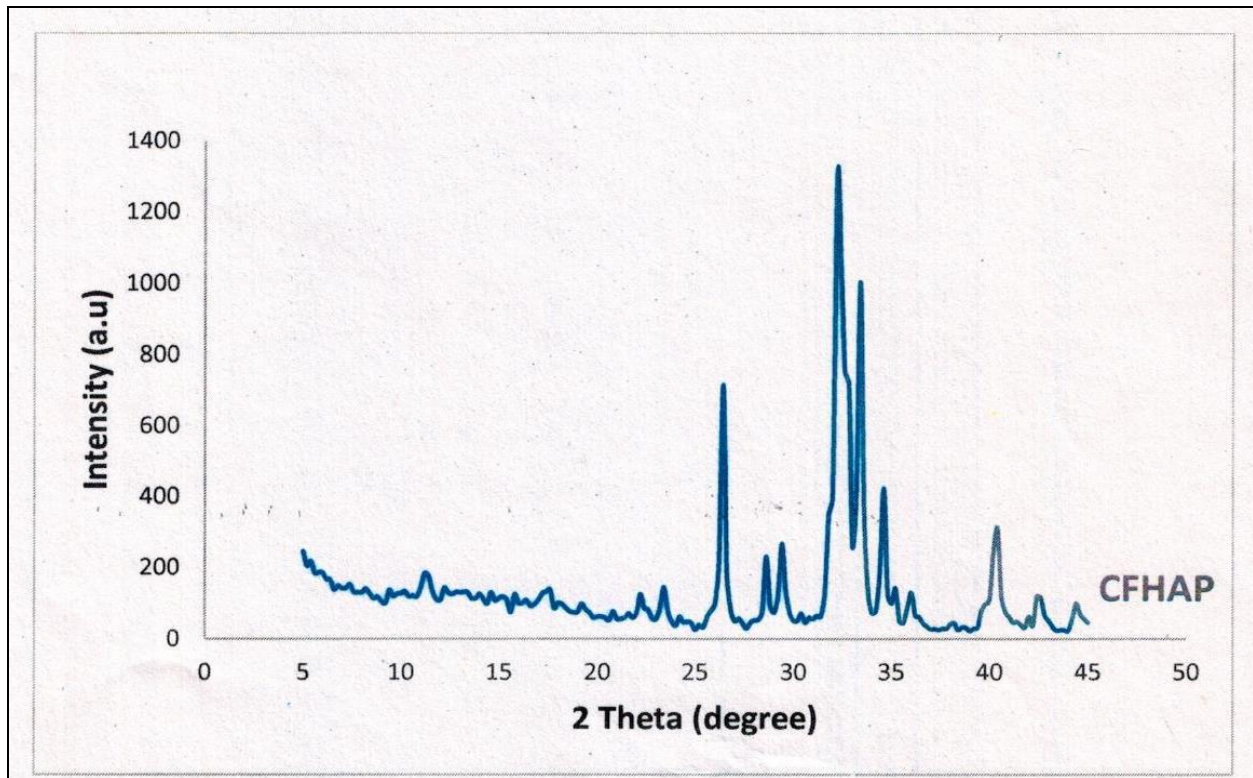


Figure 3: XRD Spectra of Crayfish Hydroxylapatite

4.4 Sem Analysis

As shown in figure 4 the SEM micrograph revealed a well-structured porous morphology showing that nHAP will be a good candidate for bone/tissue engineering.



Figure 4: SEM Micrograph Of nHAp from Crayfish Mandible (CFHAp)

The SEM micrograph of nanohydroxyapatite derived (Figure 4) from crayfish mandible revealed agglomerated, irregular nanosized particles with a rough surface morphology. Such structural features are beneficial for tissue engineering applications as they mimic the hierarchical architecture of natural bone, enhancing osteoconductivity and promoting cellular adhesion. The observed particle aggregation is consistent with high surface energy at the nanoscale, and the porous texture supports potential biointegration and nutrient transport in scaffold applications.

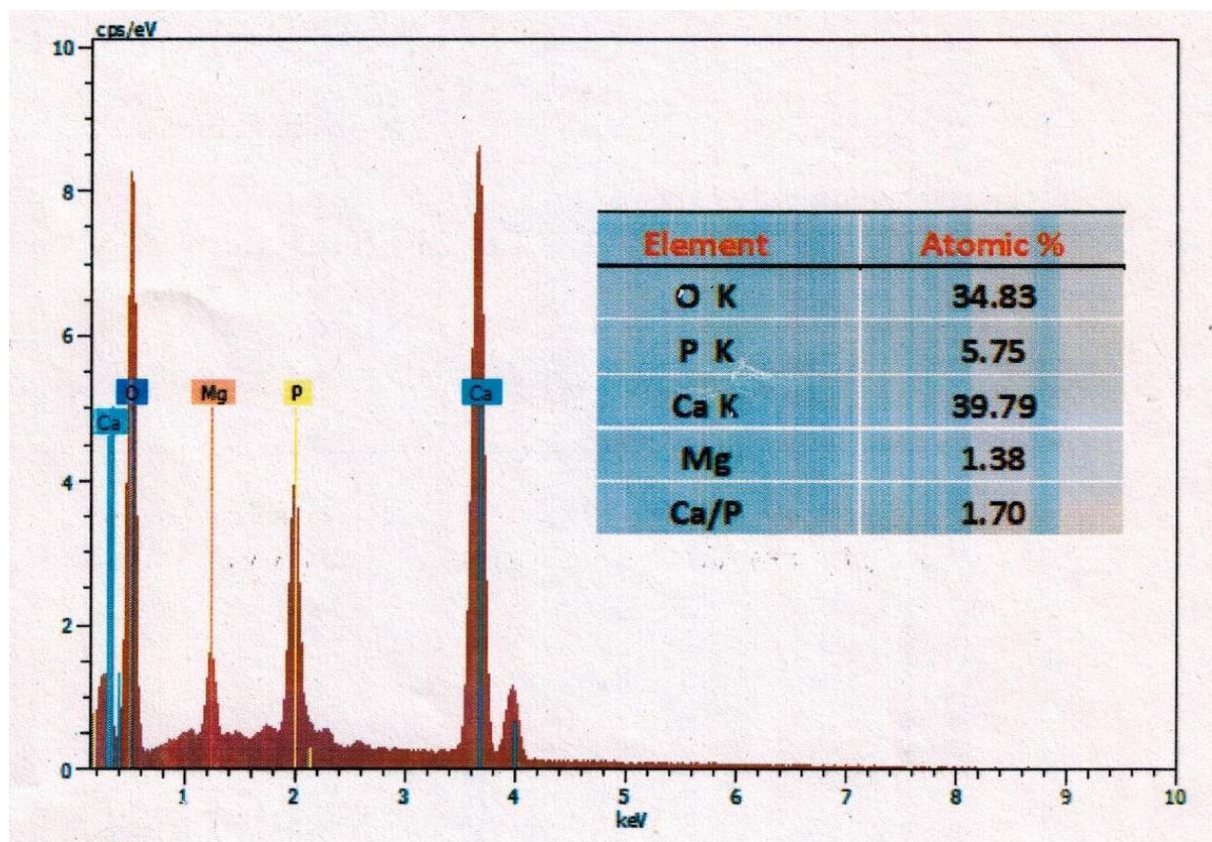


Figure 5: SEM-EDS Spectra of Crayfish Mandible (CFHAp)

Figure 5 revealed the elemental composition containing all the standard HAp elements calcium, phosphorus, oxygen and magnesium present in Ag/MgO of nanohydroxyapatite. The SEM-EDS analysis of crayfish mandible-derived nanohydroxyapatite. The figure revealed the presence of calcium (39.79 %), oxygen (34.83%), phosphorus (5.75%), and magnesium (1.38 %). The calculated Ca/P ratio of 1.70 is close to the stoichiometric hydroxyapatite value (1.67), indicating chemical similarity to natural bone mineral. The detection of magnesium suggested ionic substitution within the apatite lattice, which is known to enhance bioactivity. These findings confirm the suitability of the material for potential use in bone tissue engineering applications. The use of electrons for the study of particles has had an enormous impact, allowing us to obtain an immense amount of information about the nature, origin, and chemical composition of a research's subject (Ramirez-Leal, 2009).

4. Conclusion and Recommendation

4.1 Conclusion

CHAp powder has been developed in a cost-effective and ecofriendly method, by calcining the crayfish waste at an optimum temperature, determined through XRD analysis. It has been observed that maximum crystallinity of CHAP is obtained by calcining the crayfish waste masses at 1000°C. FT-IR and SEM-EDS analysis also confirmed the presence of calcium,

phosphate and oxygen functional groups. The conversion of bio waste to wealthy biomaterial was successfully carried out

4.2 Recommendation

Ag/MgO Nanohydroxylapatite has an antibacterial properties which would be good for the prevention of any infection with medical implants. Thus, application of the material in tissue engineering, for water purification and extraction of heavy metal and toxic ionic compound are highly recommended. Further advance characterization using FESEM, HRTEM, XPS and TGA are also recommended to ascertain additional structural and thermal properties

References

- [1] Adak, M.D., Purohit, K.M. Synthesis of nano-crystalline hydroxyapatite from dead snail shells for biological implantation, *Trends Biomater. Artif. Organs* 25(2011) 101–106.
- [2] Agarwal, H.; Kumar, S. V.; Rajeshkumar, S. A Review on Green Synthesis of Zinc Oxide Nanoparticles—an Eco-Friendly Approach. *Res. Eff. Tech.* 2017, 3, 406–413. DOI: 10.1016/j.reffit.2017.03.002.
- [3] Alorku, K.; Manoj, M.; Yuan, A. (2020). A plant-mediated synthesis of nanostructure hydroxylapatite for biomedical applications; a review. *RSC Advances*, 10(67), 40923-40939
- [4] Amanulla, A.M and Sundaram, R. “Green synthesis of TiO₂ nanoparticles using orange peel extract for antibacterial, cytotoxicity and humidity sensor applications,” *Materials Today: Proceedings*, vol. 8, pp. 323–331, 2019.
- [5] Bandeira, M.; Giovanela, M.; Roesch-Ely, M.; Devine, D. M.; da Silva Crespo, J. Green Synthesis of Zinc Oxide Nanoparticles: A Review of the Synthesis Methodology and Mechanism of Formation. *Sustain. Chem. Pharm.* 2020, 15, 100223. DOI: 10.1016/j.scp.2020.100223.
- [6] Bin, M.M., Pinky, N.S., Chowdhury, F., Md Sahadat, H., Mahmud, M., Md Saiful, Q., Jahan, S.A., Ahmed, A. Environmental remediation by hydroxyapatite: solid state synthesis utilizing waste chicken eggshell and adsorption experiment with Congo red dye, *J. Saudi Chem. Soc.* 27 (2023) 101690.
- [7] Cañon-Davila, D.F., Castillo-Paz, A.M., Londoño-Restrepo, S.M., Pfeiffer, H., Ramirez-Bon, R., Rodriguez-Garcia, M.E. Study of the coalescence phenomena in biogenic nanohydroxyapatite produced by controlled calcination processes at low temperature, *Ceram. Int.* 49 (2023) 17524–17533.
- [8] Dennyamol, P.V., Rani, J. Morphological diversity in nanohydroxyapatite synthesized from waste egg shell: verification and optimization of various synthesis parameters, *Intern. J. Sc. & Techn.* 2 (2014) 179–185.

- [9] Doan, P.M., Ngoc, D.T., Ange, N., Patrick, S. Novel one-step synthesis and characterization of bone-like carbonated apatite from calcium carbonate, *Mater. Res. Bull.* 51 (2014) 236–243.
- [10] Elshama, S. S.; Abdallah, M. E.; Abdel-Karim, R. Zinc Oxide Nanoparticles: Therapeutic Benefits and Toxicological Hazards. *TONMJ.* 2018, 5, 16–22. DOI: 10.2174/1875933501805010016.
- [11] Erdogan, O.; Abbak, M.; Demirbolat, G. M.; Birtekocak, F.; Aksel, M.; Pasa, S.; Cevik, O. Green Synthesis of Silver Nanoparticles via *Cynara Scolymus* Leaf Extracts: The Characterization, Anticancer Potential with Photodynamic Therapy in MCF7 Cells. *PLoS ONE* 2019, 14, e0216496. DOI: 10.1371/journal.pone.0216496.
- [12] Ganaie, S. U.; Rajalakshmi, R.; Abbasi, T.; Abbasi, S. Green Synthesis of Silver Nanoparticles by Coral Vine and Assessment of Their Properties. *Bioinspired Biomim. Nanobiomater.* 2019, 8, 115–129. DOI: 10.1680/jbibn.18.00019
- [13] Guerrero, C.L., Garza-Cervantes, J., Caballero-Hernández, D., González-López, R., Sepúlveda-Guzmán, R., Cantú-Cárdenas, E. Synthesis and characterization of calcium hydroxide obtained from agave bagasse and investigation of its antibacterial activity, *Rev. Int. Contam. Ambient.* 33 (2017) 347–353, <https://doi.org/10.20937/rica.2017.33.02.15>.
- [14] Habeeb, A.M., Salih, N.A. Synthesis of hydroxyapatite from egg shell bio- waste for use in functionally graded NiTi/HA bone implants, *Ann. Chimie Sci. Matériaux* 48 (2024) 57–62.
- [15] Hamidi, A., Salimi, M., Yusoff, A. Synthesis and Characterization of Eggshell-Derived Hydroxyapatite via Mechanochemical Method: A Comparative Study, *AIP Conference Proceeding*, 2017, <https://doi.org/10.1063/1.4981867>.
- [16] Hassan, M.N., Mahmoud, M.N., El-Fattah, A.A., Kandil, S. Microwave-assisted preparation of Nano-hydroxyapatite for bone substitutes, *Ceram. Int.* 42 (2016) 3725-3744. N. Iqbal, M.R.A. Kadir, N.H.B. Mahmood, M.F.M. Yusoff, J.A. Siddique, N. Salim, G.R.
- [17] Hussain, I.; Singh, N.; Singh, A.; Singh, H.; Singh, S. Green Synthesis of Nanoparticles and Its Potential Application. *Biotechnol. Lett.* 2016, 38, 545–560. DOI: 10.1007/s10529-015-2026-7.
- [18] Jaswal, A., Samir, S., Manna, A. Synthesis of nanocrystalline hydroxyapatite biomaterial from waste eggshells by precipitation method, *Trans. Indian Inst. Met.* 76 (2023) 2221–2230, <https://doi.org/10.1007/s12666-023-02937-x>.
- [19] Ibraheem, S. A., Audu, E. A., Jaafar, M., Atabat, J. A., et al. Novel pectin from *Parkia biglobosa* pulp mediated green route synthesis of hydroxyapatite nanoparticles. *Surfaces and Interfaces*, 17, 100360 (2019). DOI: 10.1016/j.surfin.2019.100360

- [20] Kumar, H., Bhardwaj, K., Dhanjal D.S. "Fruit extract mediated green synthesis of metallic nanoparticles: A new avenue in pomology applications," *International Journal of Molecular Sciences*, vol. 21, no. 22, p. 8458, 2020.
- [21] Lastra, G.; Luque, P. A.; Quevedo-Lopez, M. A.; Olivas, A. Electrical Properties of p-Type ZnTe Thin Films by Immersion in Cu Solution. *Mater. Lett.* 2014, 126, 271–273. DOI: 10.1016/j.
- [22] Leyla, K., Salahi, E., Mobasherpour, I., Rajabi, A., Javaheri, M. Characterization of nano-hydroxyapatite synthesized from eggshells for absorption of heavy metals, *Synthesis and Sintering* 3 (2023) 241–247, <https://doi.org/10.53063/synsint.2023.34190>.
- [23] Li, M., Xiong, P., Yan, F., Li, S., Ren, C., Yin, Z., Li, A., Li, H., Ji, Y. Zheng, Y. Cheng, An overview of graphene-based hydroxyapatite composites for orthopedic applications, *Bioactive Mater* 3 (2018) 1–18, <https://doi.org/10.1016/j.bioactmat.2018.01.001matlet.2014.04.058>.
- [24] Muthu, D., Kumar, G.S., Kattimani, V.S., Viswabaskaran, V., Girija, E.K. Optimization of a lab scale and pilot scale conversion of eggshell biowaste into hydroxyapatite using microwave reactor, *Ceram. Int.* 46 (2020) 25024–25034.
- [25] Ofudje, E.A., Adedapo, A.E., Oladeji, O.B., Sodiya, E.F., Ibadin, F.H., Zhang, D. Nano-rod hydroxyapatite for the uptake of nickel ions: effect of sintering behavior on adsorption parameters, *J. Environ. Chem. Eng.* 9 (2021) 105931, <https://doi.org/10.1016/j.jece.2021.105931>.
- [26] Oladoyinbo, F. O., Adekola, A. H., Ofudje, E. A., Al-Ahmary, K. M., Al-Mhyawi, S. R., Alshdoughi, I. F., Alrahili, M. R., & Alsaiani, A. A. (2024). Eggshell Derived Scaffold of Hydroxyapatite–Ammonium Bicarbonate Nano-Composite: Bioactivity and Cytotoxicity Studies. *Heliyon*, 10(17), e36493. <https://doi.org/10.1016/j.heliyon.2024.e36493>
- [27] Osuchukwu, O.A., Salihi, A., Abdullahi, I., Etinosa, P.O., Obada, D.O. A comparative study of the mechanical properties of sol-gel derived hydroxyapatite produced from a novel mixture of two natural biowastes for biomedical applications, *Mat. Chem. and Phys.* 297 (2023) 127434, <https://doi.org/10.1016/j.matchemphys.2023.127434>.
- [28] Ozgur, U.; Avrutin, V.; Morkoc, H. Zinc Oxide Materials and Devices Grown by Molecular Beam Epitaxy. In *Molecular Beam Epitaxy*, Elsevier: Massachusetts, 2018; pp. 343–375.
- [29] Poinern, G. E. J.; Brundavanam, R. K.; Thi Le, X.; Djordjevic, S.; Prokic, M.; Fawcett, D. Thermal and ultrasonic influence in the formation of nanometer scale hydroxyapatite bio-ceramic. *International Journal of Nanomedicine* 6, 2083–2095 (2011)
- [30] Ramirez-Leal, R. *Microsc. Microanal.* 15 (Suppl. 2) (2009) 1300-1301.
- [31] Sandile, M.C., Onwubu, S.C., Mokhothu, T.H., Mdluli, P.S., Mishra, A.K. Comparative assessment of the remineralization characteristics of nano-hydroxyapatite extracted from

- fish scales and eggshells, *J. Appl. Biomater. & FuncT. Mat.* 21 (2023) 22808000231180390.
- [32] Shi, D., Tong, H., Lv, M., Luo, D., Wang, P., Xu, X., Han, Z. Optimization of hydrothermal synthesis of hydroxyapatite from chicken eggshell waste for effective adsorption of aqueous Pb(II), *Environ. Sci. Pollut. Res.* 28 (2021) 58189–58205.
- [33] Shih-Ching, W., Hsueh-Chuan, H., Shih-Kuang, H., Ya-Chu, C., Wen-Fu, H. Synthesis of hydroxyapatite from eggshell powders through ball milling and heat treatment, *J. Asian Ceram. Soc.* 4 (2016) 85–90.
- [34] Singh, A.; Singh, N.; Afzal, S.; Singh, T.; Hussain, I. Zinc Oxide Nanoparticles: A Review of Their Biological Synthesis, Antimicrobial Activity, Uptake, Translocation and Biotransformation in Plants. *J. Mater. Sci.* 2018, 53, 185–201. DOI: 10.1007/s10853-017-1544-1.
- [35] Sultana, K.; Ahmad, B.; Rauf, A.; Huang, L.; Ramadan, M. Synthesis, Characterization and Pharmacological Activities of Silver Nanoparticles Using *Bistorta affinis* and *Malcolmia cabulica* Extracts. *Bioinspired Biomim. Nanobiomater.* 2020, 9, 7–15. DOI: 10.1680/jbibn.18.00012.
- [36] Sushma, N. J.; Prathyusha, D.; Swathi, G.; Madhavi, T.; Raju, B. D. P.; Mallikarjuna, K.; Kim, H. S. Facile approach to synthesize magnesium oxide nanoparticles by using *Clitoria ternatea* characterization and in vitro antioxidant studies. *Applied Nanoscience* 6, 437–444 (2016). DOI: 10.1007/s13204-015-0455-1
- [37] Tang, Y., Zhang, Y., Wei, Q., Tang, X., Zhuang, W. Biocompatible chitosan–collagen–hydroxyapatite anofibers coated with platelet-rich plasma for regenerative engineering of the rotator cuff of the shoulder, *RSC Adv.* 9 (2019) 27013–27020, <https://doi.org/10.1039/c9ra03972d>.
- [38] Toibah, A.R., Misran, F., Shaaban, A., Mustafa, Z. Effect of pH condition during hydrothermal synthesis on the properties of hydroxyapatite from eggshell waste, *J. Mech. Eng. Sci.* 13 (2019) 4958–4969, <https://doi.org/10.15282/jmes.13.2.2019.14.0411>.
- [39] Wu, S.C., Tsou, H.C., Hsu, H.K Hsu, S.K., Liou, S.P., Ho, W.F. A hydrothermal synthesis of eggshell and fruit waste extract to produce nanosized hydroxyapatite, *Ceram. Int.* 39 (2013) 8183–8188.
- [40] Zubieta-Otero, L.F., Londoño-Restrepo, S.M., Lopez-Chavez, G., Hernandez-Becerra, E., Rodriguez-Garcia, M.E. Comparative study of physicochemical properties of bio-hydroxyapatite with commercial samples, *Mater. Chem. Phys.* 259 (2021) 124201.